Cell and Tissue Research (2019) 376:401–412
https://doi.org/10.1007/s00441-019-02991-2

REGULAR ARTICLE

Identification and characterization of an antimicrobial peptide, lysozyme, from *Suncus murinus*

Shota Takemi[1] · Shiomi Ojima[1] · Toru Tanaka[2] · Takafumi Sakai[1,3] · Ichiro Sakata[1]

Received: 29 August 2018 / Accepted: 6 January 2019 / Published online: 24 January 2019

Abstract

Lysozyme is one of the most prominent antimicrobial peptides and has been identified from many mammalian species. However, this enzyme has not been studied in the order Insectivora, which includes the most primitive placental mammals. Here, we done the lysozyme cDNA from *Suncus murinus* (referred to as suncus, its laboratory name) and compare the predicted amino acid sequence to those from other mammalian species. Quantitative PCR analysis revealed a relatively higher expression of this gene in the spleen and gastrointestinal tract of suncus. The lysozyme-immunopositive (ip) cells were found mainly in the red pulp of the spleen and in the mucosa of the whole small intestine, including the follicle-associated epithelium and subepithelial dome of Peyer's patches. The lysozyme-ip cells in the small intestine were mostly distributed in the intestinal crypt, although lysozyme-expressing cells were found not only in the crypt but also in the villi. On the other hand, only a few lysozyme-ip cells were found in the villi and some granules showing intense fluorescence were located toward the lumen. As reported for other mammals, Ki67-ip cells were localized in the crypt and did not co-localize with the lysozyme-ip cells. Moreover, fasting induced a decrease in the mRNA levels of lysozyme in the intestine of suncus. In conclusion, we firstly identified the lysozyme mRNA sequence, clarified expression profile of lysozyme transcripts in suncus and found a unique distribution of lysozyme-producing cells in the suncus intestine.

Keywords Lysozyme · Suncus · Intestine · Spleen · Peyer's patch

Introduction

Antimicrobial peptides (AMPs) play a crucial role in mucosal homeostasis and confer protection against microbial pathogens. AMPs are secreted in tissues that interact with potentially harmful pathogens, such as in the epithelia of the skin, lung and gastrointestinal (GI) tract. They are well conserved in animals in which they have been reported (Ageitos et al. 2017). Lysozyme, the first antimicrobial protein discovered by Alexander Fleming in 1922 (Allison 1922), is one of the most studied AMPs that kill certain species of bacteria by hydrolyzing the peptidoglycan layer of their cell walls (Ragland and Criss 2017). The major lysozyme produced in most vertebrates, including mammals, is the C-type (chicken or conventional type) lysozyme, which has served as a model protein for comparative studies on sequence analysis and enzyme function (Callewaert and Michiels 2010). Human lysozyme was the first mammalian lysozyme to be sequenced and is known to be highly expressed in the GI tract and bone marrow (Wehkamp et al. 2006). In particular, Paneth cells located at the bottom of the crypts of the small intestine release AMPs containing lysozyme (Tobi et al. 1992). Lysozyme was also observed in the primary (azurophil) and secondary (specific) granules of bone marrow neutrophils (Cramer and Breton-Gorius 1987) and is the major secretory product of macrophages (Gordon et al. 1974). In mice, lysozyme M, an ortholog of human lysozyme, is the predominant form in most of the tissues and lysozyme P predominates in the intestinal

Electronic supplementary material The online version of this article (https://doi.org/10.1007/s00441-019-02991-2) contains supplementary material, which is available to authorized users.

✉ Ichiro Sakata
isakata@mail.saitama-u.ac.jp

[1] Area of Regulatory Biology, Division of Life Science, Graduate School of Science and Engineering, Saitama University, 255 Shimo-okubo, Sakura-ku, Saitama 338-8570, Japan

[2] Faculty of Pharmaceutical Sciences, Department of Pharmaceutical and Health Sciences, Josai University, 1-1 Keiyaki dai, Sakado, Saitama 350-0295, Japan

[3] Area of Life-NanoBio, Division of Strategy Research, Graduate School of Science and Engineering, Saitama University, 255 Shimo-okubo, Sakura-ku, Saitama 338-8570, Japan

Paneth cells (Cross et al. 1988). Lysozyme M was demonstrated to be highly expressed in macrophages, moderately expressed in the lung and small intestine and showed low expression levels in the spleen, thymus, large intestine and heart (Cross et al. 1988). In addition, lysozyme is highly expressed in human stomach (as revealed from the Human Protein Atlas, www.proteinatlas.org); however, the expression level is reported to be low in the stomach of mice (Cross et al. 1988). As described above, the tissue distribution of lysozyme is different in humans and mice, suggesting that its contribution to the innate immune system against bacterial infection is different in humans and mice. However, few studies have focused on the comparative analysis of the distribution of lysozyme in different tissues.

Recently, some studies focused on the regulatory mechanisms of lysozyme expression and secretion in the intestinal Paneth cells of mice under unusual conditions. Bel et al. (2017) showed that lysozyme is secreted through secretory autophagy, an autophagy-based alternative secretion pathway enabled during bacterial infection. In addition, an investigation using a mouse starvation model revealed that lack of feeding results in decreased lysozyme expression as well as in decreased expression of other AMPs, such as cryptdin and RegIIIγ (Hodin et al. 2011). These in vivo regulatory mechanisms in lysozyme production under different conditions, such as bacterial infection and starvation in mammalian species other than mouse, are not yet fully understood.

The musk shrew (*Suncus murinus*; suncus used as a laboratory name) is a member of the order Insectivora, which is considered as the most primitive of placental mammals (Murphy et al. 2007). Studies on lysozyme have been reported for seven orders of mammals, namely Primates, Artiodactyla, Rodentia, Lagomorpha, Carnivora, Diprotodontia and Perissodactyla (Callewaert and Michiels 2010). However, lysozyme has not yet been identified from the order Insectivora. Suncus has recently been recognized as a useful small animal model for GI motility studies because of its unique characteristics. For example, it produces the GI hormone, motilin (Tsutsui et al. 2009) and the anatomical structure of its stomach is similar to that of humans (Horn et al. 2013). In addition, it can vomit (Ito et al. 2003), an action that is usually lacking in rodents (Sanger et al. 2011). It has also been reported that in the intestine of suncus, the cecum and Paneth cells, both of which play an important role in the immune response, are absent. To date, only one study has focused on the mucosal immune system in suncus but the focus was on the function of the tonsil (Suzumoto et al. 2006). Thus, the immune system in the intestine of suncus is still unknown. In this study, we aim to determine the sequence of suncus lysozyme and to characterize the tissue distribution of lysozyme mRNA. We also observe the effect of fasting on the expression of lysozyme mRNA in the GI tract of suncus.

Materials and methods

Animals

Adult suncus of either sex (7–40 weeks old, weighing 40–110 g) of an outbred KAT strain, established from a wild population in Kathmandu, Nepal, were used. Differences in body mass index in different ages of adult suncus were not significant. The animals were housed individually in plastic cages equipped with an empty can as a nest box and were kept under controlled conditions (23 °C ± 2 °C; lights were kept on from 0800 to 2000 h) with access to water and commercial trout pellets (No. 5P; Nippon Formula Feed Manufacturing, Yokohama, Japan) ad libitum. The energy content of the pellets was 344 kcal/100 g and they contained 54.1% protein, 30.1% carbohydrate and 15.8% fat. The unfasted control group was similarly housed but the fasted group was made to fast for 24 h and the refed group was subjected to ad libitum feeding followed by fasting for 24 h. All efforts were made to minimize the suffering of animals and to reduce the number of animals used in the experiment. All procedures were approved and performed in accordance with the guidelines of the Saitama University Committee on Animal Research.

Tissue preparation

The animals were euthanized with an intraperitoneal injection of sodium pentobarbital (Tokyo Chemical Industry Co., Ltd.; 64.8 mg/mL; 0.4 mL/kg) and then, approximately 1.5-cm long sections of the stomach, five segments of the small intestine (shown in Fig. 2a) and the colon were removed. Each tissue was opened along its longitudinal axis and washed with phosphate-buffered saline (PBS; pH 7.4) to remove the gastrointestinal content. The tissue samples were collected in ISOGEN (Nippon Gene, Toyama, Japan) for RNA isolation. In addition, for immunohistochemistry (IHC) and in situ hybridization (ISH), segments were fixed for 1 day in either Bouin–Hollande solution or in 4% paraformaldehyde prepared in 0.067 M phosphate buffer (PB), pH 7.4. For IHC, the fixed tissues were dehydrated with increasing concentration of ethanol and xylene and were then embedded in Paraplast Plus (McCormick Scientific, St Louis, MO). Serial sections (7 μm thick) were subsequently made with a microtome and mounted on silane-coated glass slides (ShinEtsu Chemicals, Tokyo, Japan). For ISH, the fixed tissues were immersed in PB containing 30% sucrose for 1 day. After immersion, the tissues were embedded in Tissue Tek Compound (Sakura Finetechnical Co., Tokyo, Japan) and frozen with liquid nitrogen. Serial sections (10 μm thick) were made with a cryomicrotome and mounted onto MAS-coated glass slides (S9441; Matsunami Glass Ind., Ltd., Osaka, Japan).

Cloning of suncus lysozyme cDNA

Total RNA was extracted from all the tissue samples using ISOGEN RNA extraction reagent (Nippon Gene) according to the manufacturer's instructions. Any contamination with traces of DNA was removed by RQ1 RNase-free DNase (Promega, Madison, WI). cDNA was synthesized with 1 μg of total RNA using random primers and PrimeScript II reverse transcriptase (TaKaRa Bio, Shiga, Japan). For cloning, PCR was performed using Ex Taq (TaKaRa Bio) with the primer sets shown in Table S1. The amplification reaction was performed under the following conditions: 94 °C for 5 min, 40 cycles at 94 °C for 30 s (denaturation), 60 °C for 30 s (annealing), 72 °C for 30 s (extension) and a final extension step at 72 °C for 10 min. The PCR product was cloned into pGEM-T Easy Vector (Promega, Madison, WI) and sequencing was performed by Eurofins Genomics K.K. (Tokyo, Japan). The alignments of nucleotide and amino acid sequences were carried out using ClustalW (http://clustalw.ddbj.nig.ac.jp/).

Real-time quantitative PCR

The expression levels of lysozyme and β-actin mRNAs in different tissues were examined by real-time quantitative PCR. In order to ensure the confidence of the cDNA template, we examined the relative lysozyme expression within three housekeeping genes (β-actin, GAPDH and cyclophilin) and found that the relative lysozyme expression was consistent in each housekeeping gene tested. Thus, we demonstrated lysozyme expression relative to β-actin as a representative housekeeping gene. The primers for the different genes that were analyzed are shown in Table S1. Real-time quantitative PCR was performed using SYBR premix Ex Taq (TaKaRa Bio) according to the manufacturer's instructions. The amplification reactions were performed using a LightCycler 96 (Roche Diagnostics, Indianapolis, IN). The initial template was denatured for 30 s at 95 °C. The cycling profile was as follows: 5 s at 95 °C (denaturation) and 15 s at 60 °C (annealing and extension); 45 cycles of this profile were run. Each mRNA was quantitated with reference to a linear amplification curve obtained from serial dilutions of each PCR product. The relative amount of each mRNA was normalized to the amount of β-actin mRNA and the ratio was calculated. The amplicon size and specificity was confirmed by electrophoresis on a 2% (*w*/*v*) agarose gel and melting curve analysis, respectively.

Immunohistochemistry

Immunohistochemical detection of lysozyme cells using a polyclonal antibody against lysozyme (PA5-16668; Thermo Fisher Scientific K.K., Tokyo, Japan) was done using the avidin-biotin-peroxidase complex (ABC) method, as described in a previous report (Takemi et al. 2016). Briefly, the sections were deparaffinized with xylene and rehydrated through a descending concentration series of ethanol. The sections were treated with 0.5% sodium metaperiodate for 15 min to block the endogenous peroxidase and subsequently with 1% sodium thiosulfate for 10 min. After washing with distilled water, the sections were incubated with blocking reagent (0.4% Triton X-100 and 1% bovine serum albumin in PBS) for 2 h. Thereafter, the sections were washed with PBS and incubated overnight with rabbit anti-mouse lysozyme antibody, which was diluted 1:400 in the blocking reagent. For negative controls, the primary antibody was replaced with the blocking reagent. A second incubation with biotin-conjugated goat anti-rabbit IgG serum (Vectastain ABC kit; Vector Laboratories, Inc., Burlingame, CA), diluted 1:300 with blocking reagent, was performed for 1 h and this was followed by further washing with PBS for 15 min. Finally, the sections were incubated for 30 min with an ABC solution (Vectastain ABC kit) prepared according to the manufacturer's instructions. All the incubations were carried out in a humid chamber at room temperature. The sections were treated with 0.02% 3,3′-diaminobenzidine-tetrahydrochloride-dihydrate (DAB) mixed with 0.006% hydrogen peroxide (H_2O_2) in 0.05 M Tris-HCl, pH 7.6, for about 5 min and were then counterstained with hematoxylin. The sections were dehydrated with a graded ethanol series, cleared in xylene, mounted with Entellan medium (Merck, Darmstadt, Germany) and viewed under a light microscope (BX60; Olympus, Tokyo, Japan).

In situ hybridization

ISH was performed as described in a previous report (Takemi et al. 2016). Briefly, the sections were washed twice with RNase-free PBS and then treated with 2 μg/mL proteinase K (Merck, Darmstadt, Germany) for 30 min at 37 °C and were subsequently fixed with 4% paraformaldehyde in 0.067 M PB (pH 7.4). After washing, the sections were treated with 0.25% acetic anhydride in 0.1 M triethanolamine for 10 min, washed for 1 min, immersed in a graded series of ethanol (for 15 s each) and twice in 100% ethanol for 15 s and finally dried for 20 min. To make the digoxigenin (DIG)-labeled antisense and sense RNA probes for the suncus lysozyme, a 357-bp fragment was amplified by reverse transcription PCR (RT-PCR) using the primer pair 3 (shown in Table S1), cloned into pGEM-T Easy Vector (Promega) and labeled with an RNA labeling kit using T7 and SP6 RNA polymerase (Roche Diagnostics). The DIG-labeled sense and antisense probes were diluted to 1 ng/μL in hybridization buffer (50% formamide, 10 mM Tris-HCl, pH 7.6, 1X Denhardt's solution, 200 μg/mL tRNA, 0.1 mg/mL 10% dextran sulfate, 600 mM NaCl, 0.25% SDS and 1 mM EDTA, pH 8.0) and overlaid on the tissue sections. The sense probe was used as a negative control. The sections were then incubated for 16 h at 42 °C in a humid chamber. After incubation, the slides were

immersed in 2X SSC containing 50% formamide for 30 min. The sections were then treated with TNE [10 mM Tris-HCl (pH 7.6), 500 mM NaCl, and 1 mM EDTA (pH 8.0)] for 10 min at 37 °C and washed with 2X SSC for 20 min at 42 °C. The sections were incubated for 5 min in buffer-1 [100 mM Tris-HCl (pH 7.5), 150 mM NaCl and 0.01% Tween 20], immersed in 1.5% blocking reagent (Roche Diagnostics) in buffer-1 for 1 h at 37 °C and then incubated with an alkaline phosphatase-conjugated anti-DIG antibody (Roche Diagnostics) diluted 1:500 in buffer-1. The sections were then washed twice in buffer-1 for 15 min and in buffer-2 [100 mM Tris-HCl (pH 9.5), 100 mM NaCl and 50 mM $MgCl_2$] for 3 min. A chromogen solution [337 μg/mL 4-nitro blue tetrazolium chloride (NBT), 175 μg/mL 5-bromo-4-chloro-3-indolyl-phosphate (BCIP) in buffer-2] was added and the sections were incubated until a visible signal was detected. The chromogen reaction was stopped by adding a reaction stopping solution [10 mM Tris-HCl (pH 7.6), 1 mM EDTA (pH 8.0)]. The sections were washed with PBS, mounted with 90% glycerol in PBS and then visualized and photographed under a light microscope (BX60; Olympus).

Double immunofluorescence

For immunofluorescent double staining, the sections were boiled in a citrate antigen retrieval buffer (10 mM sodium citrate, pH 6.0) for 20 min and then pretreated with the blocking reagent for 2 h, as described above. The sections were then incubated overnight at room temperature in Ki67 monoclonal antibody (1:800 dilution; SolA15; eBioscience™) in a humid chamber and this was followed by a 2-h incubation with goat anti-mouse IgG conjugated with Alexa Fluor 488 (1:200 dilution; No. a-11001; Thermo Fisher Scientific, Fremont, CA). After washing with PBS, the sections were incubated overnight with the polyclonal lysozyme antibody, diluted 1:400 with blocking reagent and then washed with PBS. Thereafter, the sections were incubated with goat anti-rabbit IgG conjugate with Alexa Fluor 594 (1:200 dilution; No. ab150080; Abcam, Cambridge, UK) for 2 h. After washing with PBS, the slides were mounted with Vectashield Mounting Medium containing 4′,6-diamidino-2-phenylindole (DAPI; Vector Laboratories, Inc.). The images were visualized and recorded using a fluorescence microscope (BX60; Olympus).

Morphometric analysis

After taking digital photographs with a digital camera (DP70; Olympus), under a light microscope (BX60; Olympus), the number of positively stained cells per crypt section was calculated as the average cell count in three sections for each animal. For the analysis, at least 100 crypts per section were used. The individual positive cells were confirmed by nuclear staining with hematoxylin.

Statistical analysis

Data are expressed as means ± SEM. For counting lysozyme-ip cells per crypt and for real-time quantitative analysis in the fasting experiments, differences between groups were compared using one-way ANOVA, followed by pairwise comparisons using Tukey's post hoc test. Differences were considered to be statistically significant at a P value < 0.05. All statistical analyses were performed using GraphPad Prism 5.0 (GraphPad Software, Inc., San Diego, CA).

Results

Characterization of suncus lysozyme cDNA and its phylogenic analysis

The nucleotide sequence analysis showed that the open reading frame of suncus lysozyme cDNA cloned from mRNA extracted from the intestine was 447 bp, which was predicted to encode a 148-amino acid polypeptide. Comparison to other available mammalian protein sequences confirmed that the signal peptide of suncus lysozyme has 18 amino acids in the N-terminal region (Fig. 1a). The positions of eight cysteine residues, which form four disulfide bonds and participate in the process of protein folding and those of glutamic acid residue at position 35 and aspartic acid residue at position 53 in the catalytic center, were observed to be similar to those reported in other mammalian species (Fig. 1a). Based on the mRNA and amino acid sequences of lysozyme, excluding the signal peptide portion, the suncus lysozyme exhibited a high homology to the lysozymes from human (mRNA 80.1%; protein 83.1%), mouse (74.7%; 76.2%), rat (74.0%; 73.1%), dog (78.5%; 80.0%), cow (77.2%; 71.5%) and pig (78.0%; 77.7%) and a moderate homology to those from the common brushtail possums (62.6%; 60.8%) (Table 1). Phylogenic analysis revealed that the suncus lysozyme first branched in the placentarians (Fig. 1b).

Tissue distribution of lysozyme mRNA in suncus

In suncus, the border between the small and large intestines is not clear because of the absence of cecum. Thus, the intestine of suncus was divided into five segments of equivalent length of the small intestine (Fig. 2a). We performed quantitative RT-PCR analysis to investigate the tissue distribution of lysozyme mRNA in suncus (Fig. 2b). The highest concentration of lysozyme mRNA among all the tissues examined was found in the spleen, whereas a moderate level was observed in the lung, bone marrow, stomach and small intestine, wherein the expression level gradually increased from the proximal to the distal region. Lower levels of lysozyme mRNA were detected

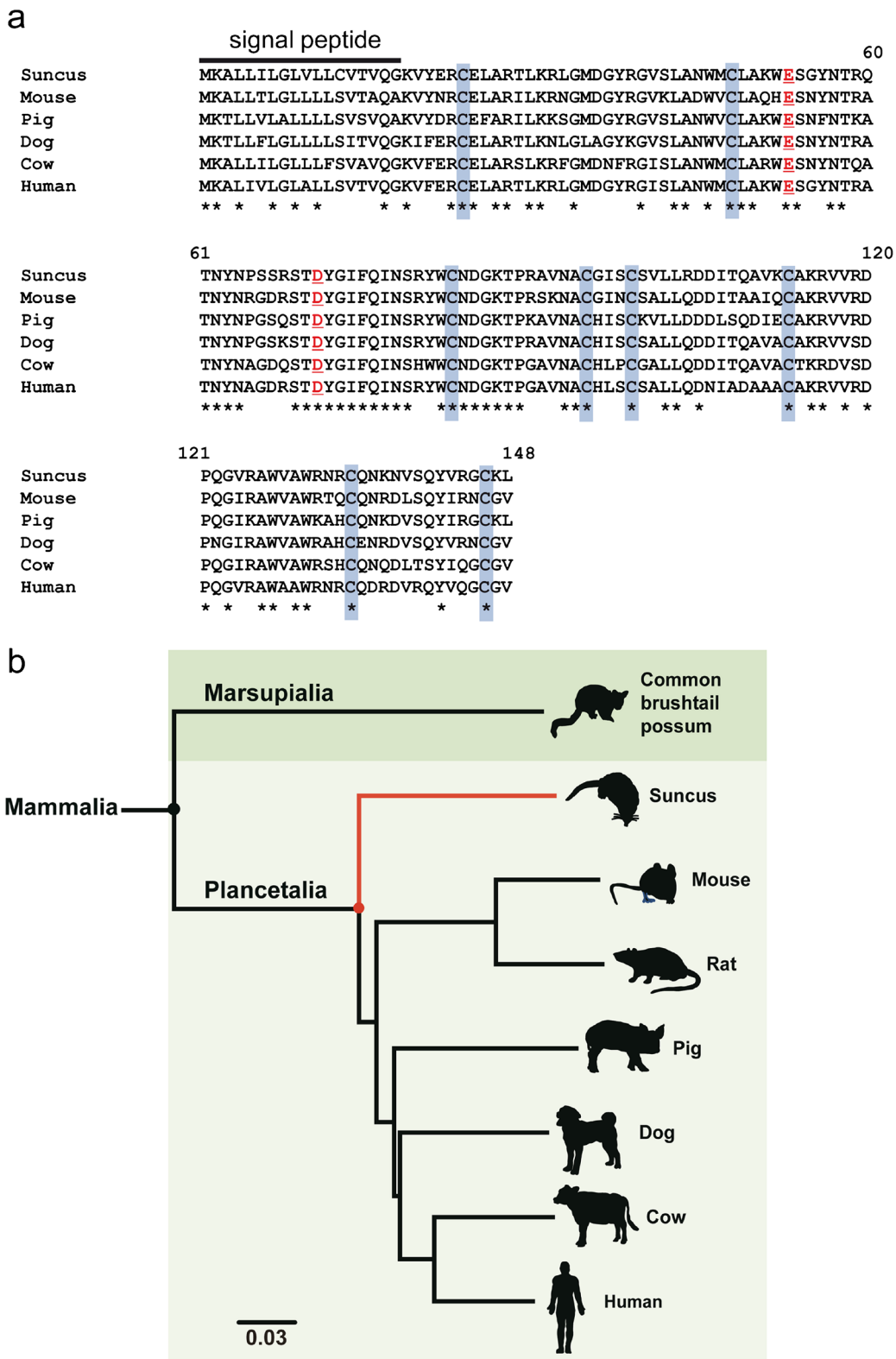

Fig. 1 Identification of the suncus lysozyme sequence. **a** Multiple sequence alignment of the deduced amino acid sequences of suncus lysozyme. Identical residues are identified by an asterisk. The conserved cysteine residues that form disulfide bonds are shaded in blue. The catalytic residues corresponding to positions 53 and 71 are shown in red and are underlined. The nucleotide and amino acid sequences are registered with the following accession numbers: mouse lysozyme C-1, NP_038618.1; pig lysozyme, AAA86644.1; dog lysozyme, AIE13825.1; cow lysozyme, AAC48683.1. **b** Molecular phylogenic tree constructed from the coding regions of lysozyme genes. The branch to *Suncus* is shown in red. Scale bar indicates substitutions/site

Table 1 Homology of the mRNA and protein sequences of suncus lysozyme to other mammalian species

Suncus vs	Human	Mouse	Rat	Dog	Cow	Pig	Common brushtail possum
mRNA	80.1% (358/447)	74.7% (334/447)	74.0% (331/447)	78.5% (351/447)	77.2% (345/447)	78.0% (344/441)	62.6% (280/447)
Protein	83.1% (108/130)	76.2% (99/130)	73.1% (95/130)	80.0% (104/130)	71.5% (93/130)	77.7% (101/130)	60.8% (79/130)

in the kidney, esophagus, thymus and colon. The ovary exhibited the lowest level of lysozyme mRNA expression whereas the expression was not observed in the central nervous system, including the cerebral cortex, hypothalamus, medulla and in some peripheral tissues, such as the liver, muscle and uterus (Fig. 2b).

Distribution of lysozyme-ip cells in the spleen of suncus

We performed immunohistochemical staining of lysozyme in the spleen, which had the highest expression among all the tissues of suncus that were examined. The red pulp of the suncus spleen contained many scatterings of the lysozyme-ip cells (Fig. 3a), whereas, few lysozyme-ip cells were detected in the marginal zone and no signal was obtained in the white pulp (Fig. 3b, c). No non-specific signals were observed in the negative control (Fig. 3d).

Distribution of lysozyme-ip cells and lysozyme mRNA-expressing cells in the GI tract of suncus

To characterize the distribution of specific cells producing lysozyme, the intestine of suncus was assessed by immunohistochemistry. The suncus lysozyme-ip cells were found mostly in the crypts of the mucosal layer throughout the suncus intestine, whereas they were not detected in all the crypts, as observed in other mammals (Fig. 4a, c, e). There were no signals in the myenteric plexus and smooth muscle layer but some signals were found in the lamina propria. In the negative controls, in which the blocking reagent was used instead of the primary antibody, no signals were obtained (Fig. 4g). In contrast to the distribution of lysozyme-ip cells, several lysozyme mRNA-expressing (lysozyme-ex) cells detected by in situ hybridization were distributed not only in the crypts but also on the apical side of the villi (Fig. 4b, d, f). No specific cells expressing the lysozyme mRNA were observed using the sense probe (Fig. 4h). Furthermore, there were no

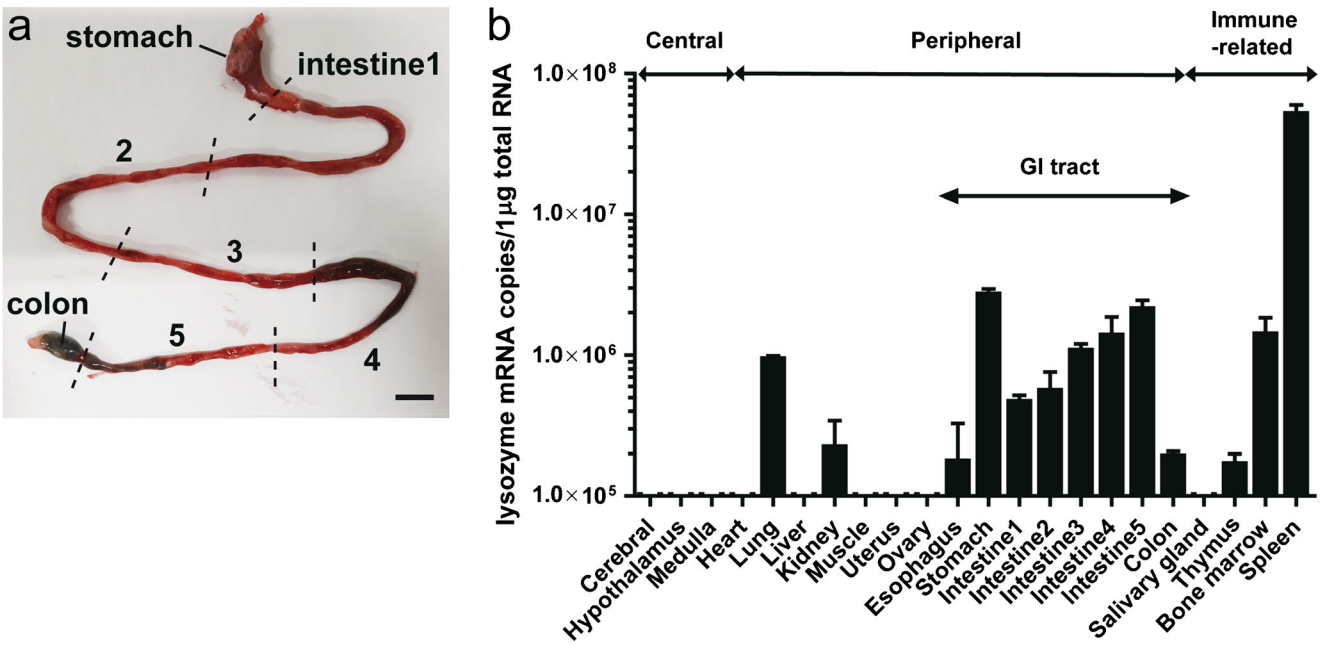

Fig. 2 Tissue distribution of lysozyme mRNA expression in suncus. **a** Representative figure of segments of the suncus gastrointestinal (GI) tract defined in this study. The small intestine of suncus was divided into five sections of equal length. **b** Real-time quantitative PCR analysis of lysozyme. The number of transcript copies is shown on a log scale. High expression was observed in the spleen followed by that in the lung, GI tract and bone marrow. Scale bars = 1 cm (**a**). Each value represents the mean ± SEM. $n = 3$

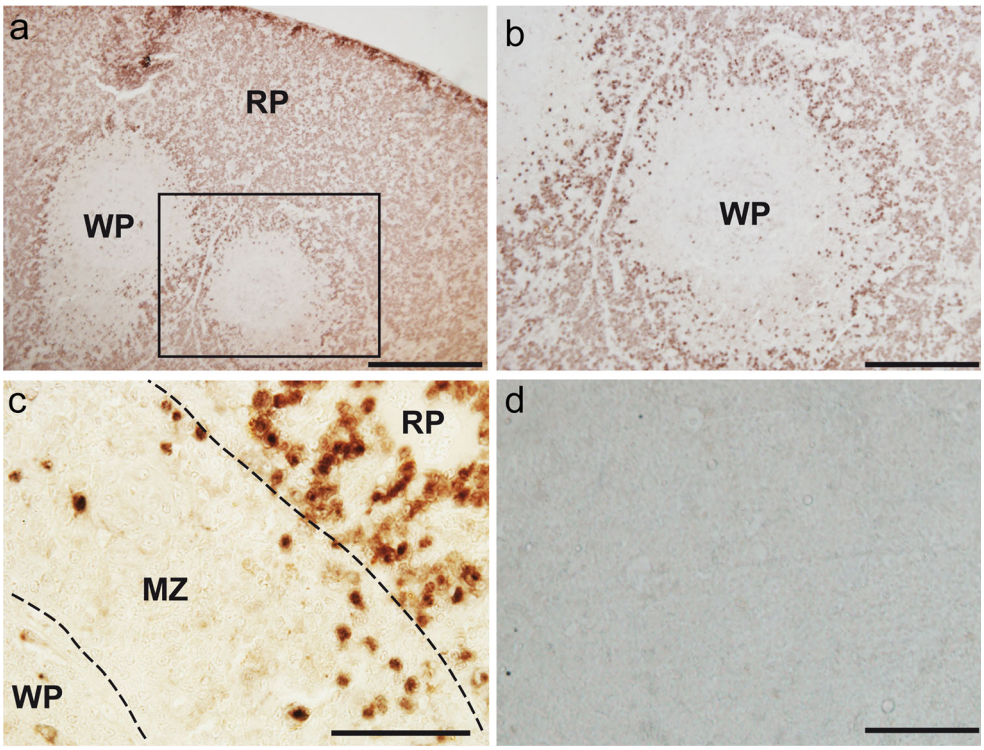

Fig. 3 Microphotographs of lysozyme-ip cells in the spleen. **a**, **b** Representative microphotographs of immunohistochemical staining for lysozyme in the spleen sections. A large number of lysozyme-ip cells were observed in the red pulp. The box shown in (**a**) indicates the field of (**b**). **c** Lysozyme-ip cells were also detected in the marginal zone. **d** Negative control. RP, red pulp; WP, white pulp; MZ, marginal zone. Scale bars = 200 μm (**a**); 100 μm (**b**); 50 μm (**c**), 200 μm (**d**)

significant differences in the number of lysozyme-ip cells per crypt between the intestines 1, 3 and 5 (Fig. 4i). Immunohistochemical analysis revealed that some granules showing intense fluorescence were located toward the lumen (Fig. 4j).

In addition, we detected Peyer's patches in the middle intestine of suncus and few lysozyme-ex cells were detected by in situ hybridization but lysozyme-ip cells were located in the subepithelial dome (SED) (Fig. 5a, b, c, arrowheads). Some lysozyme-ip cells penetrated into the follicle-associated epithelium (FAE), showing intense immunostaining signals at the epithelial surface (Fig. 5c, arrows).

Distribution of Ki67-ip cells in the suncus intestine

To understand the composition of the suncus crypt, we examined the distribution of the Ki67-ip cells, as the proliferating cells. As reported for other mammals, the Ki67-ip cells were localized in the intestinal crypt and were rarely observed in the lamina propria (Fig. 6a). On the other hand, the lysozyme-ip cells were mainly observed in the crypts of the mucosal layer and a few lysozyme-ip cells were detected in the villus (Fig. 6b). The lysozyme-ip cells in the crypts were closed-type cells (Fig. 6b′). There were no signals in the myenteric plexus and smooth muscle layer but some signals were found in the lamina propria (Fig. 6b). A small part of the Ki67-ip cells was adjacent to the lysozyme-ip cells in the small intestinal crypt of suncus (Fig. 6c, c′).

Effect of 24-h fasting and refeeding on lysozyme expression in the stomach and distal intestine of suncus

In a previous study, it was shown that Paneth cells in murine ileum exhibited decreased expression of lysozyme under starving condition (Hodin et al. 2011). To test whether the lysozyme-producing cells in suncus show similar properties to those observed in Paneth cells in mouse ileum, the suncus individuals were fasted for 24 h or fed for 1 h after 24-h fasting (refed). As observed in the mouse ileum, the relative expression of lysozyme mRNA was significantly decreased in the intestine 5 of the fasted suncus, whereas, its expression in the refed group was between the expression levels in the control and fasted groups (Fig. 7a). The number of lysozyme-ip cells per the mucosa of intestine 5 was not significantly different between the groups (Fig. 7b). The staining intensity in the lysozyme-ip cells of the fasted and refed suncus decreased upon fasting compared to that in the control (Fig. 7c–e).

Discussion

Structure of suncus lysozyme

Suncus murinus belongs to the family Soricidae of the order Insectivora, which first appeared during the Cretaceous period and is regarded as a direct ancestor of primates from a phylogenetic viewpoint (Murphy et al. 2007). In the present study, the

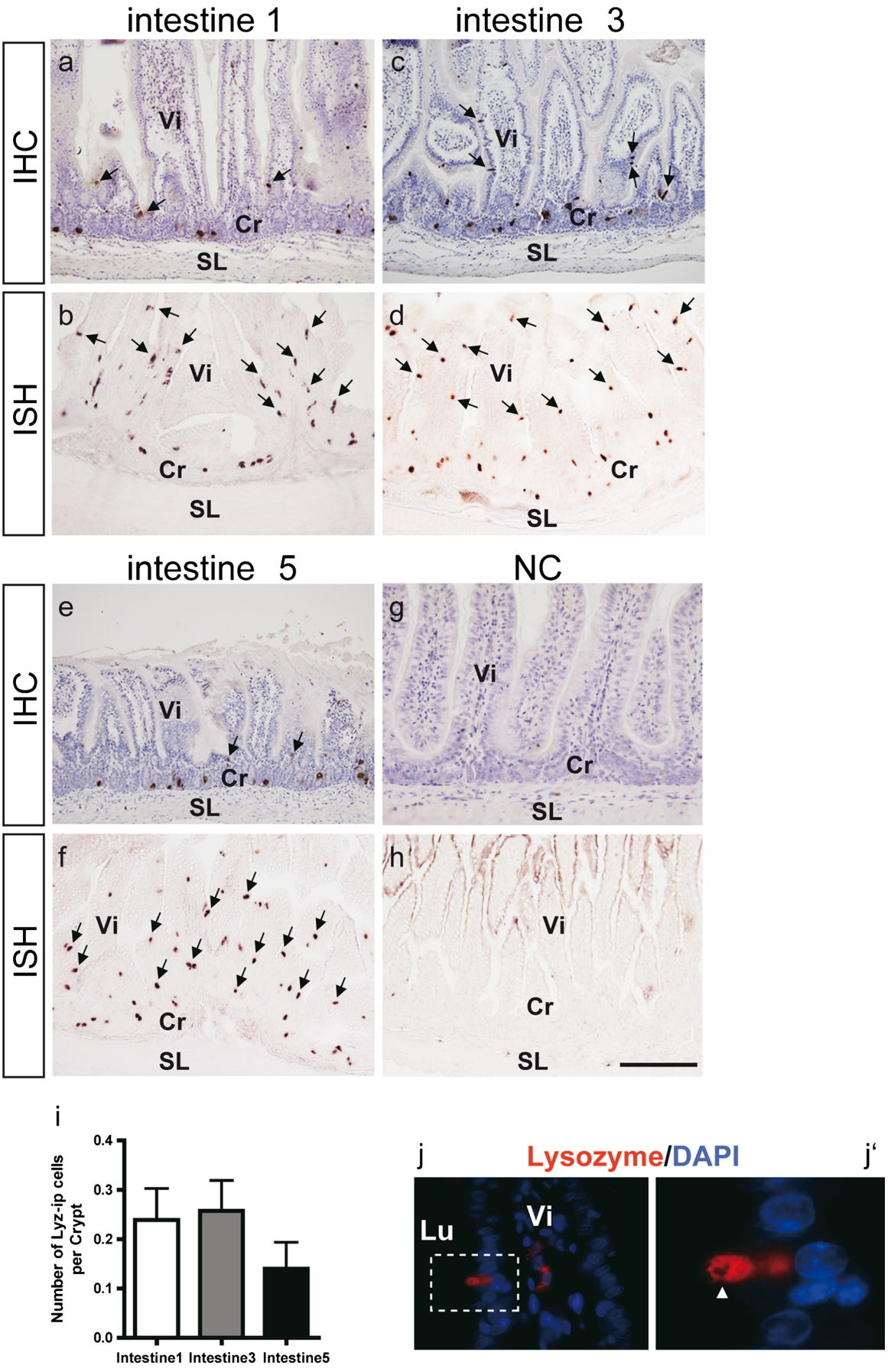
intestine 1
intestine 3
IHC
ISH
a
b
c
d
Vi
Cr
SL
intestine 5
NC
e
f
g
h
i
Number of Lyz-ip cells per Crypt
0.4
0.3
0.2
0.1
0.0
Intestine1 Intestine3 Intestine5
j
Lysozyme/DAPI
j'
Lu

Fig. 4 Lysozyme-ip cells and lysozyme-ex cells in the small intestine. Microphotographs of lysozyme-ip cells detected by immunohistochemistry (IHC) and lysozyme mRNA-ex cells detected by in situ hybridization (ISH) in intestine 1 (**a**, **b**), intestine 3 (**c**, **d**) and intestine 5 (**e**, **f**). The arrows indicate the lysozyme-ip cells located in the villi. Note that the number of lysozyme mRNA-ex cells located in the villi was more than that of the lysozyme-ip cells. In the negative controls, the blocking regent and sense probe were used in IHC (**g**) and ISH (**h**). **i** The number of lysozyme-ip cells per crypt did not alter in the different regions of the small intestine. **j** Representative figure of a lysozyme-ip cell in the villus. Some granules showing intense signals were localized toward the lumen. Vi, villi; Cr, crypt; SL, smooth muscle layer; Lu, lumen. Scale bar = 200 μm. Each value represents the mean ± SEM. $n = 3$

phylogenic tree prepared based on the similarities in the sequence of the lysozyme coding region showed almost the same branches as those found in the most recently updated mammalian phylogenies (Gomez et al. 2016) and the tree of *Suncus* was observed to branch first in Placentalia. However, the sequence of suncus lysozyme mRNA and protein exhibited high homology not only to that of humans but also to those of other mammalian species tested in this study. Among the 22 amino acids that differ between suncus and human lysozymes, the suncus lysozyme contains two more basic amino acids than that of humans, suggesting that the suncus lysozyme may exhibit a positive charge. It is generally accepted that c-type lysozymes, like human lysozymes, are cationic and can insert into and form pores in negatively charged bacterial membranes (Ragland and Criss 2017); thus, the suncus lysozyme can interact with negatively charged bacteria. In addition to its cationic nature, two important amino acid residues for the catalytic action of lysozyme (Glu-35 and Asp-53) and the residues involved in protein folding (Cys-6, -30, -65, -77, -81, -95, -116 and -128) were conserved across other mammals (for example, mice and humans).

Comparison of the distribution of suncus lysozyme mRNA with that of humans and mice

The analysis of lysozyme mRNA expression by quantitative RT-PCR demonstrated the highest levels in the spleen, followed by those in the stomach, distal intestine, bone marrow and lung, whereas weaker expression levels were observed in the kidney, esophagus, colon and thymus. In humans, the lysozyme gene is highly expressed in the GI tract, bone marrow and immune-related organs (Human Protein Atlas). On the other hand, mouse lysozyme P mRNA is abundant in the small intestine and the highest levels of lysozyme M mRNA were found in the lung and bone marrow, whereas weaker expression levels were detected in the small intestine, spleen and thymus (Cross et al. 1988). These data indicate that the tissues with high lysozyme gene expression levels in suncus were similar to those in humans and mice, except for the spleen.

Spleen lysozyme

A high level of lysozyme mRNA expression was found in the suncus spleen and lysozyme-ip cells were mainly found in the red pulp, with a few present in the marginal zone of the spleen. Macrophages are one of the major sources of lysozyme production (Cross et al. 1988); lysozyme-producing macrophages were found throughout the red pulp of the murine spleen (Keshav et al. 1991), which was similar to the distribution observed in the suncus. In addition, the lysozyme-ip cells were also observed in the red pulp of the human spleen (Human Protein Atlas). Although little is known about the distribution of lysozyme-producing cells in the spleen of various mammalian species, the results obtained in this study showed that the suncus spleen has a similar distribution of lysozyme mRNA as in humans and mice.

Differences in lysozyme distribution as assessed using ISH and IHC

In the mucosal layer of the suncus GI tract, the distribution of the lysozyme-ex cells as detected by ISH was not consistent with that of the lysozyme-ip cells as detected by IHC. The reason is assumed to be as follows: ISH detects gene

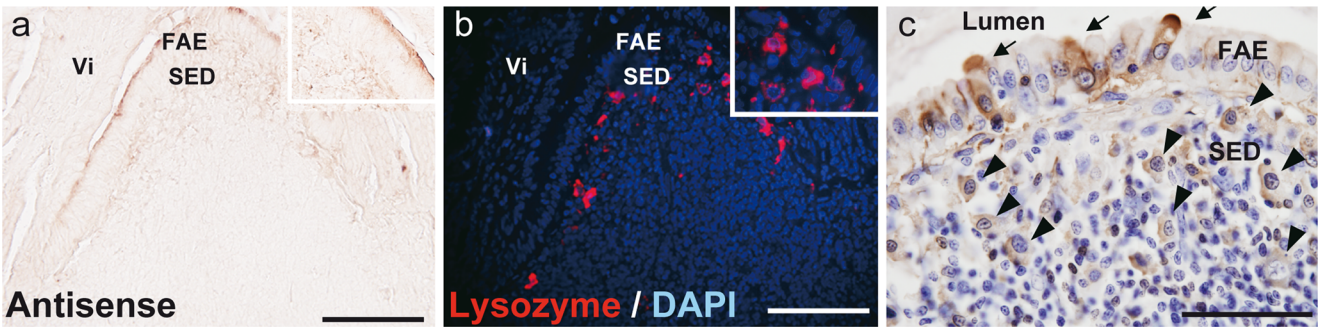

Fig. 5 Lysozyme-ex cells and lysozyme-ip cells in the Peyer's patch of the small intestine. **a**, **b** No lysozyme-ex cells were detected by in situ hybridization (ISH) but lysozyme-ip cells were found in the subepithelial dome (SED) in the section adjacent to the section shown in (**a**). **c** Lysozyme-ip cells were observed not only in the SED (indicated by arrowheads) but also in the follicle-associated epithelium (FAE) (indicated by arrows). Intense signals toward the lumen were found in the lysozyme-ip cells in the FAE. FAE, follicle-associated epithelium; SED, subepithelial dome; Vi, villus. Scale bars = 200 μm (**a**, **b**); 50 μm (**c**)

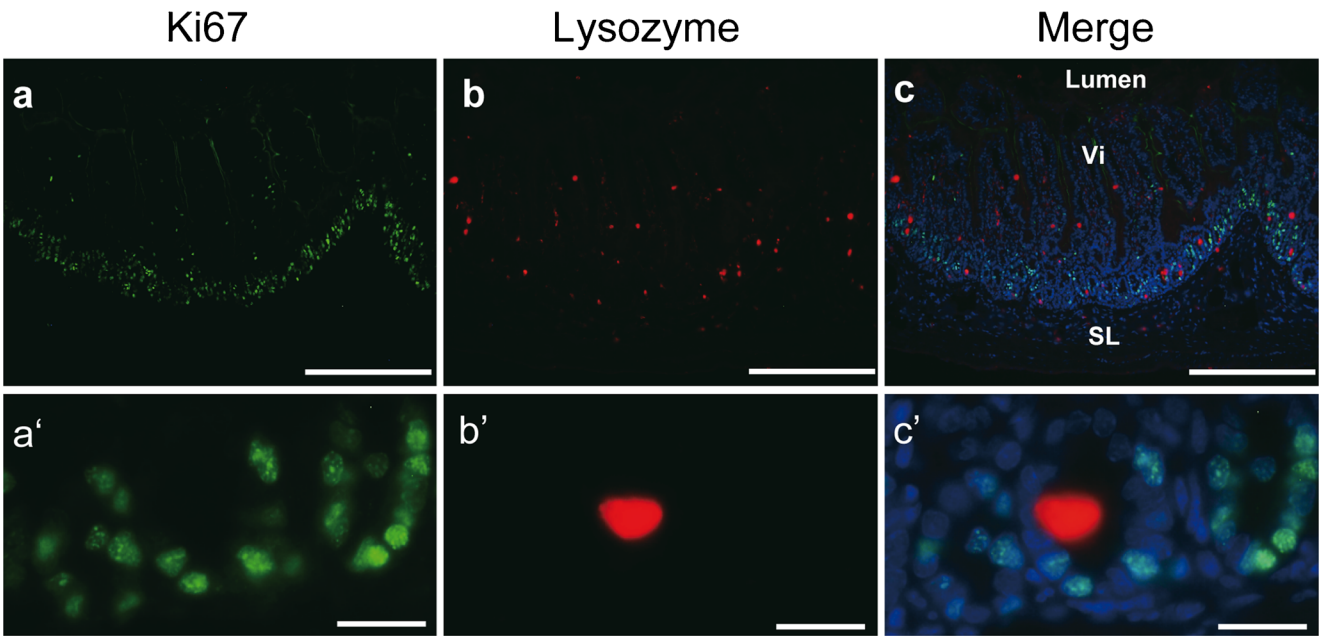

Fig. 6 Double immunostaining of lysozyme and Ki67 in the distal small intestine of suncus. **a**–**c** Ki67-ip cells were localized mainly in the crypt but a few cells were observed in the lamina propria of the villus. The Ki67-ip cells and lysozyme-ip cells were present in the mucosal layer but not in the myenteric plexus or smooth muscle layer (**a′**–**c′**). Vi, villus; SL, smooth muscle layer. Scale bars = 200 μm (**a**–**c**); 20 μm (**a′**–**c′**)

transcripts, whereas IHC detects the accumulated lysozyme protein in the cells; thus, cells that rapidly secreted the lysozyme were not detectable. However, there were a few lysozyme-ip cells in the intestinal villi, where granules

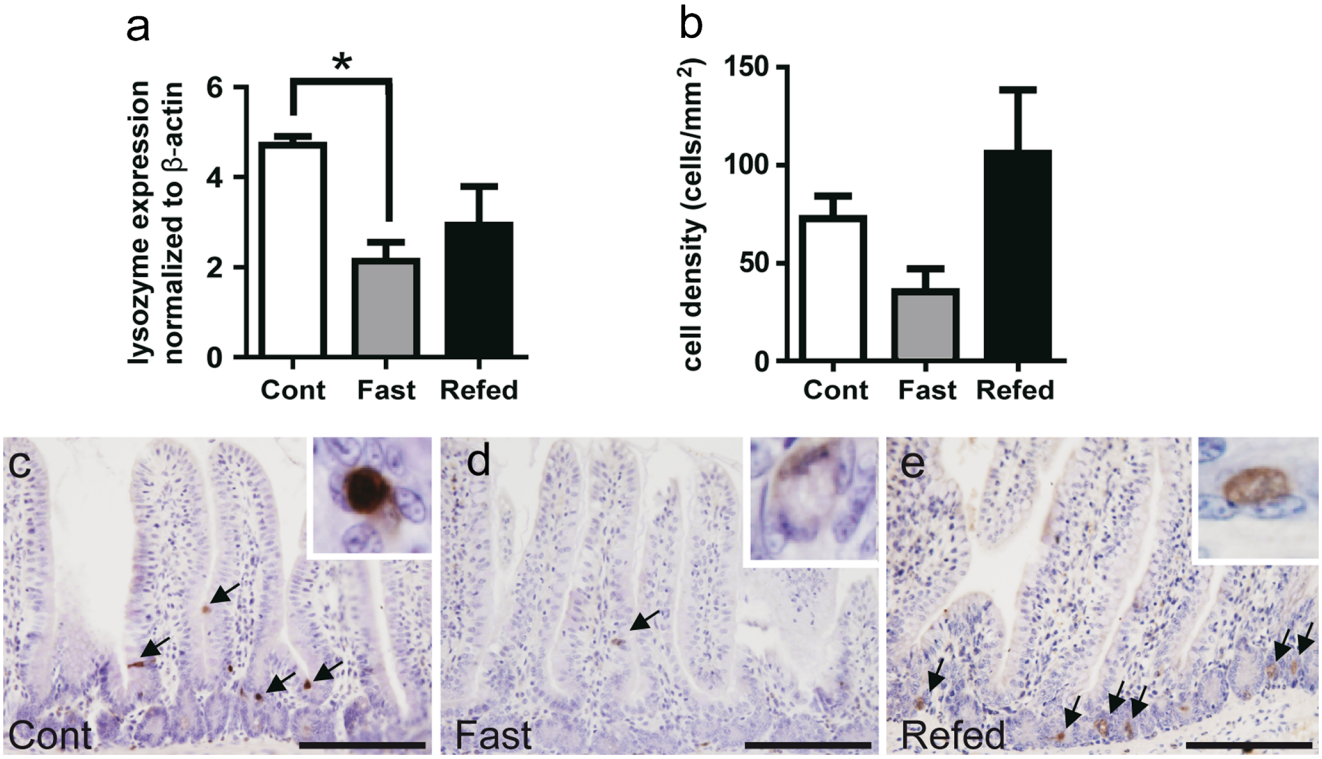

Fig. 7 Effect of fasting and refeeding on the gastrointestinal (GI) tract in suncus. **a** Expression level of lysozyme transcripts in intestine 5. The lysozyme expression level was significantly decreased in the fasted group and tended to recover after the refeeding treatment. **b** Lysozyme-ip cell number per the mucosa of intestine 5 was not significantly different between the groups. Immunohistochemical analysis of lysozyme in the control (**c**), fasted (**d**) and refed (**e**) groups showed decreased immunoreactivity in the fasted and refed groups compared to that in the control. Each value represents the mean ± SEM. $n = 3$. $^*P < 0.05$

showing intense immunofluorescence signals were located toward the lumen (Fig. 4j). In addition, these characteristics of inclination of lysozyme-ip granules toward the lumen were also detected in the Peyer's patches in suncus. These results suggested that the intestinal lysozyme is secreted into the lumen in a constitutive manner. Furthermore, lysozyme-ip cells were observed; however, lysozyme-ex cells were rarely detected in the SED of suncus Peyer's patches. Given that it has been previously reported that the SED of Peyer's patches of mouse, rat and human contain a unique population of intestinal dendritic cells or macrophages that store high levels of lysozyme (Lelouard et al. 2010), we speculate that lysozyme-ip cells detected in the SED are dendritic cells or macrophages. Intestinal dendritic cells or macrophages are known to be derived from bone marrow and store a proportion of antimicrobial factors, including lysozyme, within granules; thus, the gene transcription of antimicrobial factors would not be so active.

Characterization of lysozyme-ip cells in the GI tract of suncus

It is well known that lysozyme is located in Paneth cells in intestine in most of the mammalian species, including humans (Klockars and Reitamo 1975), mice (Satoh et al. 1988), rat (Klockars and Osserman 1974), guinea pigs (Vasquez Cachay et al. 2014) and horses (Takehana et al. 1998). Additionally, recent studies have reported that Paneth cells in pigs and chickens—which had not been previously confirmed to exist—were observed in the intestines (van der Hee et al. 2018; Wang et al. 2016). However, the distribution of the lysozyme-ip cells in the intestine of suncus was different from that in the mammals reported so far. In the suncus intestine, although the lysozyme-ip cells were found mostly in the crypt, the number of lysozyme-ip cells per crypt was about 0.1–0.2 in intestine 1 (proximal small intestine) to intestine 5 (distal small intestine). In contrast, the number of lysozyme-ip cells (defined as Paneth cells) per crypt was reported to be approximately five in the murine ileum (Shanahan et al. 2014). It is known that Paneth cells are found at the base of the crypts and produce not only antimicrobial products (e.g., lysozyme, secretory phospholipase A2, α-defensin) but also other factors that contribute to the formation of the stem cell niche (e.g., epidermal growth factor, transforming growth factor α and Wnt3). Moreover, the PAS (periodic acid-Schiff) technique positively stains Paneth cell granules as well as goblet cell premucin droplets (Lewin 1969). We performed immunohistochemical detection of lysozyme with PAS staining and confirmed that relatively few lysozyme-ip cells in the suncus intestine had PAS-positive granules (data not shown). Therefore, there is a possibility that a proportion of the lysozyme-ip cells in the crypt are Paneth cells. However, expression analysis of the cells should be performed before this can be accurately determined. On the other hand, lysozyme-ip cells in the villi were not co-localized with PAS-positive cells, suggesting that lysozyme-ip cells are not goblet cells.

We next observed the distributed cell relationship between the lysozyme-ip cells and Ki67-ip proliferative cells, because there are Ki67-ip crypt base columnar cells flanked by lysozyme-ip Paneth cells in mice (Potten et al. 2009). It was demonstrated that Ki67-ip cells were localized in the crypt of the intestine in suncus, as reported for other mammals, indicating that cell proliferation in the crypt of the intestine of suncus is equivalent to that observed in mice. Collectively, these findings imply that the regulatory system maintaining a stem cell niche in the crypt is independent of Paneth cells in suncus.

Effect of fasting and refeeding

It is well known that fasting affects the systemic metabolic condition in mammals (Longo and Mattson 2014). In the present study, fasting on suncus distal small intestine decreased lysozyme expression. This may be partly due to free fatty acids included in the diet and bacterial exposure derived from diet pellets on intestinal lumen. Indeed, several studies report that free fatty acids modulate antimicrobial peptide expression and that luminal bacteria induce the expression of antimicrobial peptides, including lysozyme in humans (Sunkara et al. 2012). However, further studies are necessary to clarify the relationship between diet components and lysozyme expression.

Conclusion

The present study demonstrates the unique characteristics of lysozyme production in suncus, such as its tissue distribution and the distribution of lysozyme-producing cells in the intestine. The distribution of other antimicrobial peptides produced from Paneth cells (for example, α-defensins and secretory phospholipase A2 group IIA) should be investigated in the future. In addition, the lysozyme expression in suncus was found to fluctuate according to the feeding conditions. Future studies are needed to address the physiological mechanisms regulating the expression of lysozyme in the intestine.

Compliance with ethical standards

Conflict of interest The authors declare that they have no conflict of interest.

Publisher's Note Springer Nature remains neutral with regard to jurisdictional claims in published maps and institutional affiliations.

References

Ageitos JM, Sanchez-Perez A, Calo-Mata P, Villa TG (2017) Antimicrobial peptides (AMPs): ancient compounds that represent novel weapons in the fight against bacteria. Biochem Pharmacol 133:117–138

Allison AFVD (1922) Observations on a bacteriolytic substance ("lysozyme") found in secretions and tissues. Br J Exp Pathol 3: 252–260

Bel S, Pendse M, Wang Y, Li Y, Ruhn KA, Hassell B, Leal T, Winter SE, Xavier RJ, Hooper LV (2017) Paneth cells secrete lysozyme via secretory autophagy during bacterial infection of the intestine. Science 357:1047–1052

Callewaert L, Michiels CW (2010) Lysozymes in the animal kingdom. J Biosci 35:127–160

Cramer EM, Breton-Gorius J (1987) Ultrastructural localization of lysozyme in human neutrophils by immunogold. J Leukoc Biol 41:242–247

Cross M, Mangelsdorf I, Wedel A, Renkawitz R (1988) Mouse lysozyme M gene: isolation, characterization, and expression studies. Proc Natl Acad Sci U S A 85:6232–6236

Gomez JM, Verdu M, Gonzalez-Megias A, Mendez M (2016) The phylogenetic roots of human lethal violence. Nature 538:233–237

Gordon S, Todd J, Cohn ZA (1974) In vitro synthesis and secretion of lysozyme by mononuclear phagocytes. J Exp Med 139:1228–1248

Hodin CM, Lenaerts K, Grootjans J, de Haan JJ, Hadfoune M, Verheyen FK, Kiyama H, Heineman E, Buurman WA (2011) Starvation compromises Paneth cells. Am J Pathol 179:2885–2893

Horn CC, Kimball BA, Wang H, Kaus J, Dienel S, Nagy A, Gathright GR, Yates BJ, Andrews PL (2013) Why can't rodents vomit? A comparative behavioral, anatomical, and physiological study. PLoS One 8:e60537

Ito H, Nishibayashi M, Kawabata K, Maeda S, Seki M, Ebukuro S (2003) Induction of Fos protein in neurons in the medulla oblongata after motion- and X-irradiation-induced emesis in musk shrews (Suncus murinus). Auton Neurosci 107:1–8

Keshav S, Chung P, Milon G, Gordon S (1991) Lysozyme is an inducible marker of macrophage activation in murine tissues as demonstrated by in situ hybridization. J Exp Med 174:1049–1058

Klockars M, Osserman EF (1974) Localization of lysozyme in normal rat tissues by an immunoperoxidase method. J Histochem Cytochem 22:139–146

Klockars M, Reitamo S (1975) Tissue distribution of lysozyme in man. J Histochem Cytochem 23:932–940

Lelouard H, Henri S, De Bovis B, Mugnier B, Chollat-Namy A, Malissen B, Meresse S, Gorvel JP (2010) Pathogenic bacteria and dead cells are internalized by a unique subset of Peyer's patch dendritic cells that express lysozyme. Gastroenterology 138:173–184 e171–173

Lewin K (1969) Histochemical observations on Paneth cells. J Anat 105: 171–176

Longo VD, Mattson MP (2014) Fasting: molecular mechanisms and clinical applications. Cell Metab 19:181–192

Murphy WJ, Pringle TH, Crider TA, Springer MS, Miller W (2007) Using genomic data to unravel the root of the placental mammal phylogeny. Genome Res 17:413–421

Potten CS, Gandara R, Mahida YR, Loeffler M, Wright NA (2009) The stem cells of small intestinal crypts: where are they? Cell Prolif 42: 731–750

Ragland SA, Criss AK (2017) From bacterial killing to immune modulation: recent insights into the functions of lysozyme. PLoS Pathog 13:e1006512

Sanger GJ, Holbrook JD, Andrews PL (2011) The translational value of rodent gastrointestinal functions: a cautionary tale. Trends Pharmacol Sci 32:402–409

Satoh Y, Ishikawa K, Tanaka H, Oomori Y, Ono K (1988) Immunohistochemical observations of lysozyme in the Paneth cells of specific-pathogen-free and germ-free mice. Acta Histochem 83: 185–188

Shanahan MT, Carroll IM, Grossniklaus E, White A, von Furstenberg RJ, Barner R, Fodor AA, Henning SJ, Sartor RB, Gulati AS (2014) Mouse Paneth cell antimicrobial function is independent of Nod2. Gut 63:903–910

Sunkara LT, Jiang W, Zhang G (2012) Modulation of antimicrobial host defense peptide gene expression by free fatty acids. PLoS One 7: e49558

Suzumoto M, Hotomi M, Fujihara K, Tamura S, Kuki K, Tohya K, Kimura M, Yamanaka N (2006) Functions of tonsils in the mucosal immune system of the upper respiratory tract using a novel animal model, Suncus murinus. Acta Otolaryngol 126:1164–1170

Takehana K, Masty J, Yamaguchi M, Kobayashi A, Yamada O, Kuroda M, Park YS, Iwasa K, Abe M (1998) Fine structural and histochemical study of equine Paneth cells. Anat Histol Embryol 27:125–129

Takemi S, Sakata I, Apu AS, Tsukahara S, Yahashi S, Katsuura G, Iwashige F, Akune A, Inui A, Sakai T (2016) Molecular cloning of ghrelin and characteristics of ghrelin-producing cells in the gastrointestinal tract of the common marmoset (Callithrix jacchus). Zool Sci 33:497–504

Tobi M, Maliakkal B, Zitron I, Alousi M, Goo R, Nochomovitz L, Luk G (1992) Adenoma-derived antibody, Adnab-9 recognizes a membrane-bound glycoprotein in colonic tissue and effluent material from patients with colorectal neoplasia. Cancer Lett 67:61–69

Tsutsui C, Kajihara K, Yanaka T, Sakata I, Itoh Z, Oda S, Sakai T (2009) House musk shrew (Suncus murinus, order: Insectivora) as a new model animal for motilin study. Peptides 30:318–329

van der Hee B, Loonen LMP, Taverne N, Taverne-Thiele JJ, Smidt H, Wells JM (2018) Optimized procedures for generating an enhanced, near physiological 2D culture system from porcine intestinal organoids. Stem Cell Res 28:165–171

Vasquez Cachay ME, Gomez EP, Rodriguez Gutierrez JL, Lira Mejia B, Perez NF, Zanuzzi CN, Barbeito C (2014) Paneth cell identification in the small intestine of Guinea pig offsprings (Cavia porcellus). Anat Rec (Hoboken) 297:856–863

Wang L, Li J, Li J Jr, Li RX, Lv CF, Li S, Mi YL, Zhang CQ (2016) Identification of the Paneth cells in chicken small intestine. Poult Sci 95:1631–1635

Wehkamp J, Chu H, Shen B, Feathers RW, Kays RJ, Lee SK, Bevins CL (2006) Paneth cell antimicrobial peptides: topographical distribution and quantification in human gastrointestinal tissues. FEBS Lett 580: 5344–5350